

The repeating microlensing event OGLE-2003-BLG-095: A plausible case of microlensing of a binary source

Matthew J. Collinge

Princeton University Observatory, Princeton, New Jersey 08544
collinge@astro.princeton.edu

ABSTRACT

The apparently repeating microlensing event OGLE-2003-BLG-095 is analyzed. Data were obtained from the OGLE Internet archive and exist in the public domain. The source is relatively bright, with an unmagnified (but possibly blended) *I*-band magnitude of 15.58, and the signal-to-noise ratio of the data is excellent. The light curve shows two distinct, smooth peaks characteristic of a double microlensing event. It can be modeled as either (1) microlensing by a binary lens or (2) microlensing of a binary source, with the latter model providing a statistically superior fit. However due to apparent low-amplitude variability of the source, the interpretation is somewhat ambiguous. OGLE-2003-BLG-095 is only the second possible case in the literature for microlensing of a well-resolved binary source.

Subject headings: binaries: general — gravitational lensing

1. Introduction

Gravitational microlensing surveys were originally suggested by Paczyński (1986) as a means of detecting dark matter in the Galaxy in the form of massive compact objects, commonly abbreviated as MACHOs following Griest (1991). Various efforts were undertaken to search for such objects, including the Optical Gravitational Lensing Experiment (OGLE; Udalski et al. 1992), the MACHO project (e.g., Alcock et al. 1993), and several others. Currently ongoing projects, most notably OGLE and MOA (Bond et al. 2001), are detecting hundreds and dozens of new microlensing events each year, respectively. The new events found by these groups are made public in real time to maximize scientific gain by enabling follow-up of interesting objects by the astronomical community.

In addition to the possibility of detecting dark matter MACHOs, microlensing surveys also offer the interesting opportunity to study the populations of stellar lenses (which constitute at least a significant fraction of all events) and sources. Since most stars are located

in multiple systems, many microlensing events show deviations from the standard Paczyński (point lens, point source) light curve. For example, some events show the effects of caustic crossings (Mao & Paczyński 1991; Gould & Loeb 1992); this provides clear evidence of lens binarity and can be used to constrain the combination of the distances to the source and lens, the source-lens relative motion, and the physical extent of the source, as well as revealing the mass ratio of the lens system. A small additional fraction of microlensing events should show clear signatures of source binarity in multiple peaks and color shifts; this fraction was estimated to be 2–5% by Griest & Hu (1992). To date no convincing example of such an event has been reported in the literature; the best case is MACHO-96-BLG-4, but the light curve of this event can be equally well fit by a binary source or binary lens model, with the binary lens providing the most natural interpretation (Alcock et al. 2000). Several authors (Dominik 1998; Han & Jeong 1998; Di Stefano 2000) have proposed explanations for the lack of such clear binary source microlensing events. Essentially, a variety of different effects including blending, unequal luminosity of binary components, and simple coincidence conspire to make most binary source microlensing light curves resemble single source, single lens events. A handful of other events, such as MACHO-96-LMC-2 Alcock et al. (2001), show signatures of binary orbital motion of the source; in this particular case, it is not clear whether both components of the binary contribute significantly to the total source flux. In any case the light curves of such events do not match the expectation of having multiple distinct, well-resolved peaks as described above.

This work analyzes the light curve of OGLE-2003-BLG-095, which shows two distinct microlensing peaks. The light curve can be fit by a binary lens or a binary source model; however, the binary source model is statistically preferred. The light curve is presented in §2, §3 contains a description of the models and fitting procedure, and the results are analyzed in §4.

2. OGLE data

An *I*-band light curve of OGLE-2003-BLG-095 was obtained from the OGLE Internet archive¹ (cf. Udalski et al. 2003), and is shown in Figure 1. The source is located at $(\alpha_{J2000}, \delta_{J2000}) = (17:59:03.04, -27:11:19.8)$; a finding chart is also available from the OGLE web site. The data set consists of 109 observations from three observing seasons spanning a period of 2.2 yr, from August 2001 through 17 October 2003. The light curve from the 2001 and 2002 observing seasons (seasons I and II hereafter) is relatively constant (to within $\pm 3\%$

¹<http://sirius.astro.uw.edu.pl/~ogle/>

excluding the highest point and the lowest point), with a mean I -band magnitude of 15.58. However, due to the high stellar surface number density in the field, some blending seems likely. The light curve from the 2003 season (III) shows two very distinct smooth peaks, with maximum magnification factors of ≈ 1.9 and ≈ 1.7 . For both peaks, the rise and fall in source intensity are well covered by observations.

In order to simplify the fitting procedure, the light curve was converted to units of relative flux by adopting the mean intensity from seasons I and II as the base flux level. Thus the mean relative flux from seasons I and II is unity by construction. Even for relatively bright sources like the one in consideration, the photometric error estimates reported by the OGLE data reduction pipeline (cf. Udalski et al. 2002) are typically somewhat too small to account for the observed scatter in the light curves of sources that do not vary intrinsically (B. Paczyński 2004, private communication). In the OGLE-2003-BLG-095 light curve from seasons I and II, the standard deviation s in flux is larger than the mean quoted error $\bar{\sigma}$ by a factor $s/\bar{\sigma} = 2.65$, a ratio which nevertheless is significantly too large to be readily explained by underestimation of uncertainties. This is probably an indication that the source (or at least one component of it, if it is a blend) is variable at the level of at least a few percent. A careful inspection of the season II light curve indicates that variations are correlated from night to night. However, no periodic signal is present at a level of significance above 50% in a Lomb-Scargle normalized periodogram (cf. Press et al. 1992; Schwarzenberg-Czerny 1998) computed for seasons I and II.

Such non-periodic variability substantially complicates the modeling process, causing greatest confusion for model effects that produce variations with similar amplitudes and time scales. See §4 for further discussion. To aid in interpreting fit results, the errors were scaled so that χ^2 per degree of freedom ν (DOF), also known as the reduced χ^2 and denoted χ_ν^2 , is unity for a constant fit to the light curve from seasons I and II. This required scaling all relative flux errors by a factor of 2.49. The scaling factor is similar to the ratio $s/\bar{\sigma}$ quoted in the previous paragraph; the fact that these two quantities differ could either be attributed to a non-Gaussian error distribution (which seems likely given the apparent systematic variations) or to the limited number of data points.

3. Modeling the light curve

Since the intensity of the source during seasons I and II was taken to be constant, microlensing models were applied to the 50 data points from season III only. Two classes of models were considered: (1) models with a coplanar binary lens consisting of two point masses, in which the source was taken to be a small (but finite) disk of uniform surface

brightness (“binary lens” or “double lens” models); (2) models with a single point mass lens and two distinct point sources (“binary source” or “double source” models). The source was treated as finite in the former case due to the possibility of caustic crossings; although there is no direct evidence of such in the OGLE-2003-BLG-095 light curve, the possibility was considered in order not to restrict the exploration of parameter space (e.g., a case in which a brief caustic crossing event occurs in a gap between observations). In the latter case, such caution was not needed since the smooth, low-magnification light curve precludes any possibility of very small (close to zero) impact parameters.

The light curve of OGLE-2003-BLG-095 suggests that the two binary components (whether of the lens or of the source) are separated by an angular distance of at least twice the angular Einstein radius θ_E . For a typical value of $\theta_E \approx 0.5$ milli-arcseconds (mas) and a distance to the binary (lens or source) of at least a few kiloparsecs (kpc), which is very likely for an event in the direction of the Galactic bulge, the implied projected separation of binary components is several Astronomical Units (AU). Assuming the masses to be not too different from a Solar mass (M_\odot), the minimum orbital period of the system is several years. Therefore, both classes of models were restricted to the static case; that is, any relative motion of binary components (lens or source) was neglected.

3.1. Parallax effect

For both classes of models, two parameters are needed to characterize the vector microlens parallax $\boldsymbol{\pi}_E$ (e.g., Gould 2000). One parameter can be chosen to be the parallax magnitude π_E , whose inverse gives the projected size \tilde{r}_E of the Einstein radius in the observer plane. A second parameter ψ then gives the lens-source proper motion angle on the sky (measured counter-clockwise from North). Following the method recently proposed by Gould (2003), all parallax fitting is done in geocentric reference frames defined with respect to the position and velocity of Earth at times very close to one of the light curve peaks.

3.2. Binary lens model

Binary lens models are characterized by eight parameters, in addition to the two components of the microlens parallax. Four parameters describe the trajectory of the lens relative to the source: the time t_0 of closest approach to the more massive binary component (corresponding roughly to one of the two event maxima), the Einstein time scale t_E , the angle ϕ between the lens line of centers and the lens trajectory with respect to the source position,

and the impact parameter u_0 to the more massive binary component. The remaining four parameters describe the lens and source properties: the binary mass ratio q and separation a , the fraction f_{bl} of the baseline intensity due to the source, and the ratio of the angular source radius to the angular Einstein radius, $\xi_{\star, \text{E}} \equiv \theta_{\star}/\theta_{\text{E}}$. All length scales (a, u_0) are in terms of the Einstein radius r_{E} of a lens with mass equal to the total mass of the binary.

For events in which it has been possible to measure or estimate the ratio $\xi_{\star, \text{E}}$ due to caustic crossings, typical values for microlensing toward the Galactic bulge are found to be on the order of 0.001–0.01 (Alcock et al. 2000; Jaroszyński 2002). In the absence of caustic crossings and at low magnification, as in the case of OGLE-2003-BLG-095, binary lens model light curves are very insensitive to the precise value of $\xi_{\star, \text{E}}$ provided it is smaller than a few tens of percent. Hence this parameter is poorly constrained by the available data, and its value is fixed at 0.01 in the subsequent analysis.

For a binary lens the model flux can conveniently be found numerically for a given lens-source configuration by finding the (multiple) image locations for a set of points on the source boundary (e.g., Gould & Gaucherel 1997). This procedure gives 3–5 new sets of points defining the image boundaries, depending on whether the source is outside, crossing, or inside a caustic. Since the surface brightness of the source is taken to be constant, the magnification is given by the ratio of the sum of the (appropriately signed) areas enclosed by the image boundaries to the area of the source.

3.3. Binary source model

The static binary source model is constructed from a linear combination of two point lens, point source models with Einstein time scales and vector parallaxes constrained to be the same for each source component. This model has seven parameters in addition to parallax: two for the fraction of the baseline intensity due to each source ($f_{\text{bl}, i}$, where $i = 1, 2$), three for the trajectory (u_0, t_0, ϕ as in the previous case except that the reference point is defined by the closest approach of the lens to the source responsible for the first peak in the light curve), source separation a , and the Einstein time scale t_{E} .

The model flux $m(t)$ at time t can be expressed as

$$m(t) = 1 + \sum_{i=1}^2 f_{\text{bl}, i} [A(u_i) - 1] \quad (1)$$

where

$$A(u) = \frac{u^2 + 2}{u(u^2 + 4)^{1/2}} \quad (2)$$

gives the total magnification for a point source, point lens system with separation u (in units of r_E). In this parametrization, the condition $f_{bl,1} + f_{bl,2} \leq 1$ must clearly be met in order for the model to be physically meaningful.

3.4. Fitting procedure

The χ^2 -minimization was performed using MINUIT, a function minimization package available as part of the CERN program library². For each class of models, the fitting algorithm was initialized in several different realizations with different sets of initial parameter values. All such sets were chosen to produce an initial model light curve that was qualitatively similar to the observed one (two well-separated smooth peaks with approximately the correct amplitude and width). For the binary lens model, four different initial source trajectories were chosen: two in which the source encountered the more massive lens first; two in which the source encountered the less massive lens first. For each of these pairs, one trajectory was chosen to pass in between the two lenses, and one was chosen not to pass in between the two lenses. The initial values of the other parameters were chosen appropriately to reproduce qualitatively the light curve shape for each of these cases. For the binary source model, an equivalent variety of initial parameter guesses were used, subject again to the requirement that the model light curve be qualitatively similar to the observations. After the best fit solutions were obtained for models in which the parallax was fixed at zero, full nine parameter fits (including parallax) were performed using the previous solutions as the initial guesses.

3.5. Fitting results

The best fit no-parallax model light curves and fit residuals are shown in Figure 2. Tables 1 and 2 contain the best fit results for the binary lens and binary source models, respectively. For the same number of DOF, the no-parallax double source model is preferred over the no-parallax double lens model by a highly significant margin of $\Delta\chi^2 = 13.3$, and furthermore this model satisfies the criterion that $\chi^2_\nu \approx 1$ (with the caveat that the overall error scaling is rather uncertain). However, the lower panels of Figure 2 both show evidence of systematic residuals, indicating that unmodeled complexity is present in both fits. This is not at all surprising in light of the evidence for low-amplitude source variability mentioned in §2, and considering that parallax has been neglected.

²<http://cernlib.web.cern.ch/cernlib/index.html>

Including the parallax effect adds two more free model parameters and results in $\Delta\chi^2 = -25.7$ and $\Delta\chi^2 = -16.5$ for the binary lens and binary source models, respectively. These large $\Delta\chi^2$ values formally indicate that the parallax effect is detected with a high level of statistical significance. The inclusion of parallax brings both models into the $\chi^2_\nu < 1$ regime, for the adopted error scaling. It also reduces the difference in the statistical quality of the two model fits, though the double source model remains superior by $\Delta\chi^2 = 4.15$ for the same number of DOF.

It is worthwhile to note that although the overall error scaling is rather arbitrary as discussed in §2 (and hence the precise value of χ^2 is far from rigorous), $\Delta\chi^2$ is still a meaningful quantity. The low values of $\chi^2_\nu = 0.783$ and $\chi^2_\nu = 0.682$ respectively obtained for the best fit double lens and double source models indicate that the errors have probably been scaled by too large a factor, resulting in values of χ^2 that are systematically low. In principle, the errors could be rescaled so that $\chi^2_\nu = 1$ for the best fitting model, but this does not seem warranted, especially in view of the complications introduced by the likely source variability. Regardless, if the errors had been scaled by a smaller factor, $\Delta\chi^2$ values would increase correspondingly.

Additionally, there are a number of degeneracies in the problem that are important to consider. In the absence of parallax, that is, when the apparent lens-source relative trajectory is (modeled as being) strictly linear, there are two fully degenerate binary lens models and four fully degenerate binary source models. The degenerate models differ only by the sign of the impact parameter u_0 and the orientation angle ϕ . There are only two equivalent binary lens solutions because trajectories on which the two lens components pass on opposite sides of the source produce fundamentally different light curves (due to proximity to caustics) from trajectories on which the two lens components pass on the same side of the source. The same does not hold for the binary source models, and hence in this case there exist four degenerate trajectories.

These degeneracies are somewhat alleviated when the parallax effect is included. For the binary lens model the degeneracy is broken; the two solutions separate by $\Delta\chi^2 = 2.79$ (only the preferred solution is given in Table 1). For the binary source model the degeneracy is largely broken as well; only the solution with the lowest χ^2 is given in Table 2. The three solutions not included in Table 2 all fall within the range $1 < \Delta\chi^2 < 2$ of the preferred solution. Regardless, the differences among these near-degenerate solutions are largely immaterial, since the best fit parameters (neglecting the sign of the impact parameter u_0 and the orientation angle ϕ) lie within or very near the $1\text{-}\sigma$ error ranges quoted in Tables 1 and 2. For all the solutions, the parallax magnitudes π_E are consistent within $1\text{-}\sigma$ with the values from the best fit solutions.

There is a further possible degeneracy discovered recently by Gould (2003). This “jerk-parallax” degeneracy can produce multiple parallax solutions for a given sign of the impact parameter. In an effort to find any such solutions, a detailed search of the π_E plane was performed for the double source model (which is more computationally tractable than the double lens model). The results are shown in Figure 3. No fully degenerate solution is present, although the contours are highly elongated in a direction perpendicular to the projected acceleration vector of Earth at the time of the first event maximum, when the geocentric reference frame is defined (as expected for this degeneracy). Numerical searches for other parameter combinations that produce similar trajectories were also performed (by solving eqs. 12–14 from Gould 2003) for both classes of models. No further degenerate solutions were discovered.

4. Discussion

An extremely relevant question is whether the parallax effect can be disentangled from the likely variability of the source (regardless of whether the variability is inherent or due to a hitherto unrecognized systematic effect). To address this issue, Figure 4 compares the deviations from constant flux in the season II light curve with the magnitude of the effect of parallax on the model light curves for season III. It is apparent that the modulations of the model light curves due to the parallax effect have similar amplitudes and variation time scales to the observed variability of the source, rendering the parallax measurements rather untrustworthy.

Further support for the notion of “contaminated” parallax measurements comes from examining the implications of the best fit parallax-included models. There is a simple relationship between the projected Einstein radius \tilde{r}_E , the lens mass M , and the lens-source relative distance $D_{\text{rel}} \equiv (D_l^{-1} - D_s^{-1})^{-1}$, where D_l and D_s are the distances from the observer to the lens and source; this relation is given by

$$D_{\text{rel}} = \frac{c^2 \tilde{r}_E^2}{4GM} \quad (3)$$

(Gould 2000). It is plausible to assume the source to be located in the Galactic bulge at a distance of approximately 8 kpc and to assume the lens to have a total mass of approximately one Solar mass. Substituting the measured values of π_E from the best fit binary lens and binary source models, one obtains $D_{\text{rel}} \approx 0.25$ kpc and $D_{\text{rel}} \approx 0.06$ kpc, respectively. In both cases $D_{\text{rel}}^{-1} \gg D_s^{-1}$, indicating that $D_l \approx D_{\text{rel}}$. Even accounting for the substantial additional uncertainties introduced by assuming the lens mass and source distance, such a nearby lens seems unlikely.

Since the apparent variability of the source limits the degree to which the binary lens and binary source models can be statistically distinguished, a definitive interpretation of OGLE-2003-BLG-095 will probably require further observations. At the least, future OGLE observations of the source will allow better constraints on its variability. A simple (though not necessarily straightforward) test which might clearly confirm the binary source model could be performed through moderate resolution optical spectroscopy to see if the source exhibits double absorption lines or radial velocity variations. An alternative possibility would be to obtain deep, high resolution imaging of the field to see if the lens can be observed directly.

5. Conclusion

The light curve of OGLE-2003-BLG-095 shows two well-separated smooth peaks that can be modeled as either microlensing by a binary lens or microlensing of a binary source. Both models are physically plausible and can possibly be tested by future observations of the source and/or lens. The binary lens model provides a more familiar explanation of the event since such phenomena have been observed many times in the past, while the binary source model is preferred on statistical grounds. Given the apparent low-amplitude variability of the source (or at least one component of it) however, statistical distinctions of the magnitude that separate the two models are somewhat suspect, especially considering the improbably large microlens parallaxes indicated by the best fit models. Despite these complications, OGLE-2003-BLG-095 remains a plausible candidate for microlensing of a well-resolved binary source – one of only two such observed to date.

The author wishes to thank B. Paczyński and T. Sumi for helpful comments and suggestions, M. Jaroszyński for providing routines (originally developed by S. Mao) to calculate binary lens light curves, A. Gould for helpful discussion, and the OGLE collaboration for making microlensing data publicly available in real time. This research was supported in part by a NDSEG Fellowship award to the author.

REFERENCES

- Alcock, C., et al. 1993, *Nature*, 365, 621
- Alcock, C., et al. 2000, *ApJ*, 541, 270
- Alcock, C., et al. 2001, *ApJ*, 552, 259

- Bond, I. A. 2001, MNRAS, 327, 868
- Di Stefano, R. 2000, ApJ, 541, 587
- Dominik, M. 1998, A&A, 333, 893
- Gould, A. 2000, ApJ, 542, 785
- Gould, A. 2003, astro-ph/0311548
- Gould, A., & Gaucherel, C. 1997, ApJ, 477, 580
- Gould, A., & Loeb, A. 1992, ApJ, 396, 104
- Griest, K. 1991, ApJ, 366, 412
- Griest, K., & Hu, W. 1992, ApJ, 397, 362
- Han, C., & Jeong, Y. 1998, MNRAS, 301, 231
- Jaroszyński, M. 2002, AcA, 52, 39
- Mao, S., & Paczyński, B. 1991, ApJ, 374, 37
- Paczynski, B. 1986, ApJ, 304, 1
- Press, W. H., Teukolsky, S. A., Vetterling, W. T., & Flannery, B. P. 1992, *Numerical Recipes* (Cambridge Univ. Press, Cambridge)
- Schwarzenberg-Czerny, A. 1998, MNRAS, 301, 831
- Udalski, A., et al. 1992, AcA, 42, 253
- Udalski, A., et al. 2002, AcA, 52, 1
- Udalski, A., et al. 2003, AcA, 53, 291

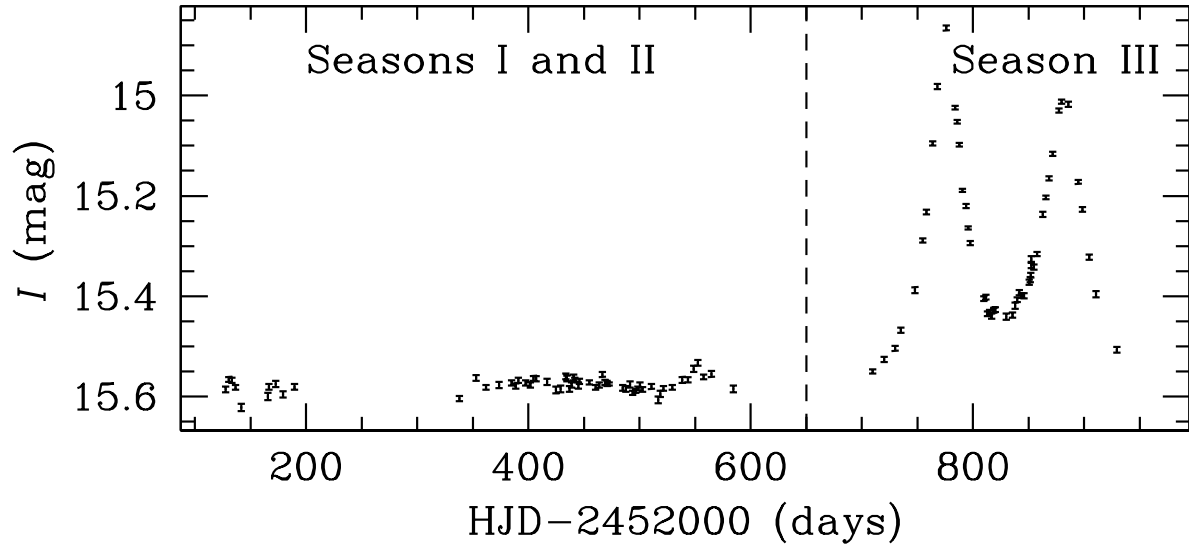


Fig. 1.— I -band light curve of OGLE-2003-BLG-095 with nominal uncertainties from the OGLE data reduction pipeline. The observing seasons referred to in the text are labeled. The source is relatively constant during the first two seasons, with the deviations due to microlensing confined to the third season.

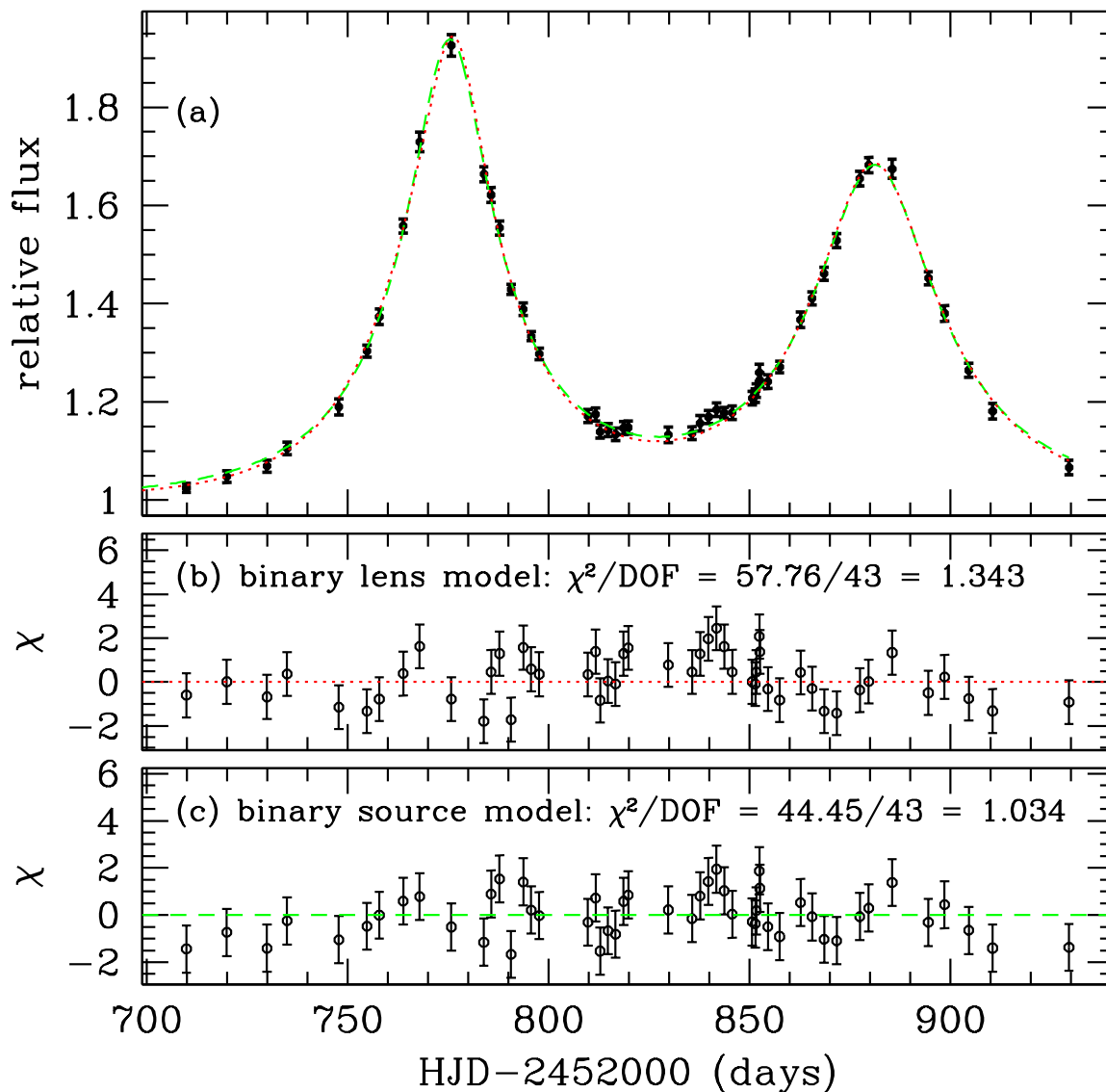


Fig. 2.— Panel (a): Best fit no-parallax binary lens (dotted curve) and binary source (dashed curve) models for the light curve of OGLE-2003-BLG-095. To the eye, there is little difference in the qualities of the two fits. Panel (b): Fit residuals in units of sigmas for the best fit binary lens model (not including parallax). Panel (c): Same as panel (b), but for the binary source model. The residuals in both of the lower panels display a somewhat systematic character.

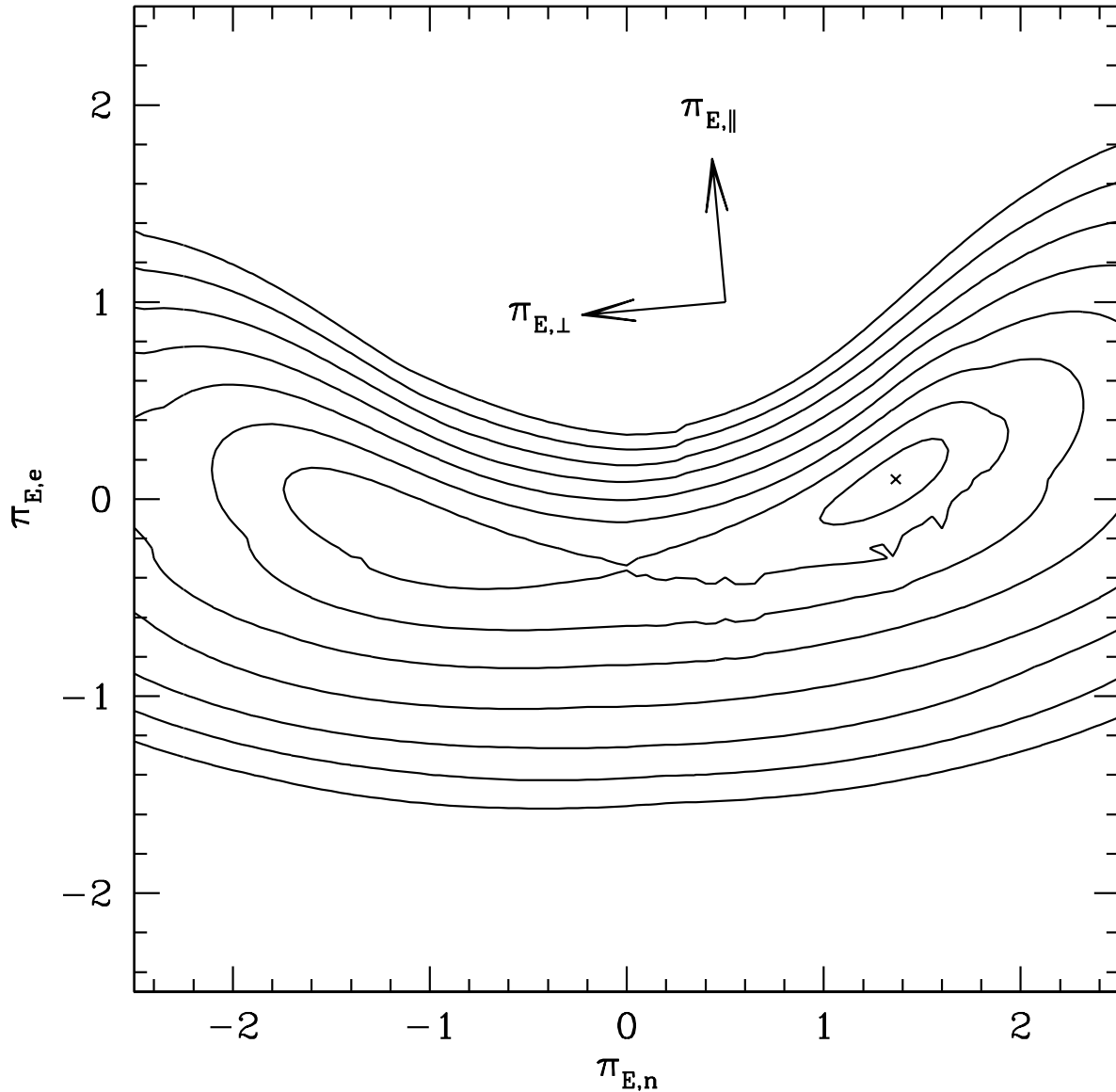


Fig. 3.— χ^2 contours in the π_E plane for the double source model. ‘X’ marks the best fit solution; contours corresponding to $\Delta\chi^2 = 1, 4, 9, 16, 25, 36, 49, 64$ are shown. The subscripts n, e refer to the North and East components of the parallax vector. The symbols \parallel and \perp refer to the projected direction of the Earth’s acceleration vector at the time of the first event maximum (which is the reference point of the geocentric frame in which parallax fitting is done). Although the contours are elongated in the expected direction, no fully degenerate solution is found as in Gould (2003).

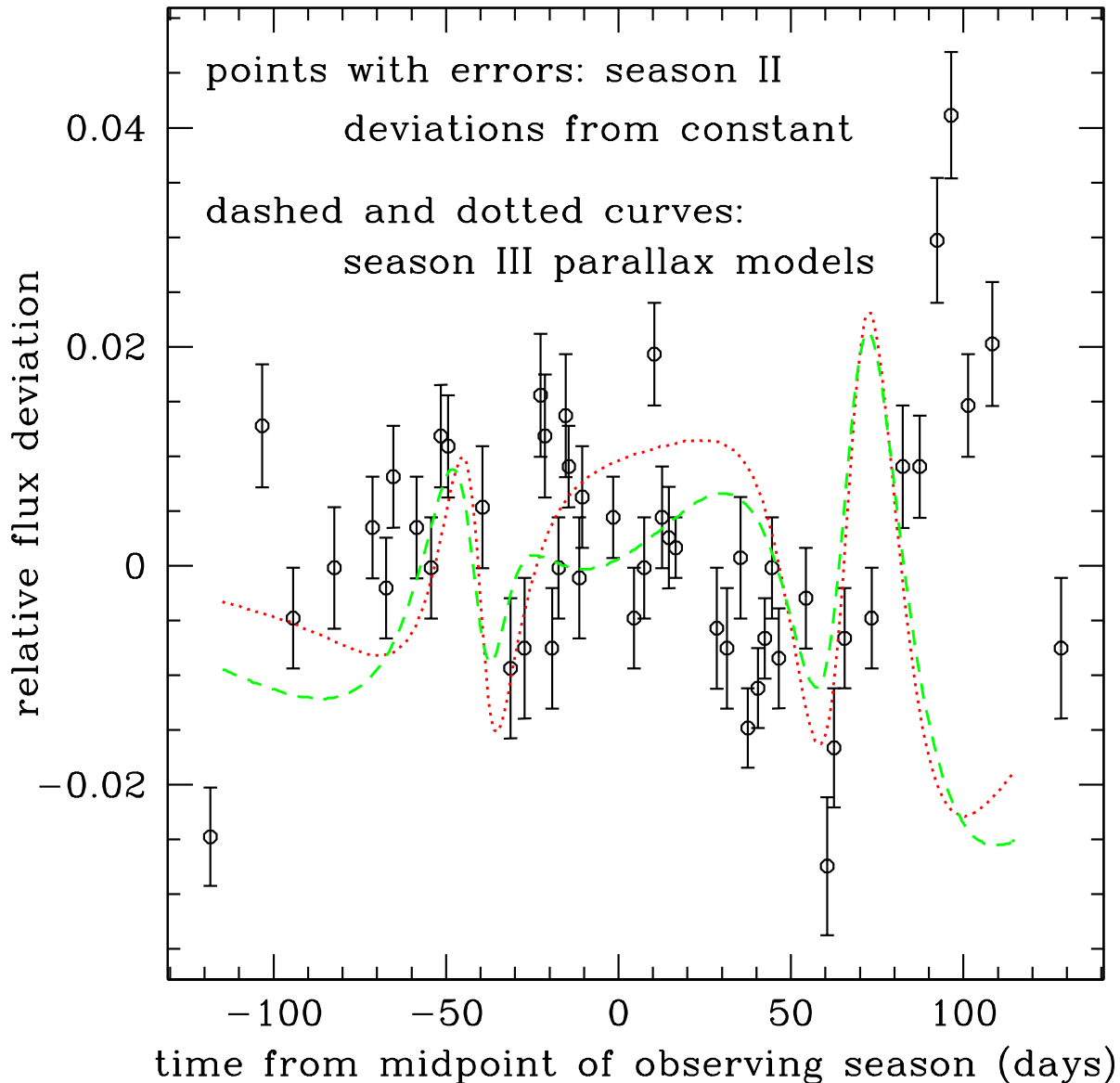


Fig. 4.— The curves do not represent fits to the data. Points with errorbars show deviations from constant relative flux from season II with nominal OGLE data reduction pipeline uncertainties. The dotted line is the binary lens parallax-included fit minus no-parallax fit from season III; the dashed line is the same, but for the binary source model. The qualitative similarities between the season II light curve and the season III “model-difference” curves are striking, especially considering that they refer to different observing seasons. The time scales for variation are similar, and notably, the amplitude of deviations from constant flux during season II is comparable to or greater than the differences between the parallax-included and no-parallax fits, even though no scaling has been applied to account for the fact that the source was brighter during season III (and thus relative flux deviations due to intrinsic source variability should be magnified as well).

Table 1. Parameters of best fit double lens model

Quantity	No-parallax best fit value	Parallax included best fit value	Units
π_E	0.0 ^a	0.7 ± 0.2	AU ⁻¹
ψ	0.0 ^a	$-0.2^{+0.2}_{-0.4}$	rad
q	1.28 ± 0.05	1.3 ± 0.1	...
a	2.90 ± 0.07	3.1 ± 0.1	r_E
ϕ	$0.048^{+0.005}_{-0.004}$	$0.25^{+0.06}_{-0.07}$	rad
u_0	-0.49 ± 0.02	$-0.51^{+0.03}_{-0.02}$	r_E
t_0	884.3 ± 0.3	884.5 ± 0.5	days ^b
t_E	39 ± 1	38 ± 2	days
f_{bl}	$0.92^{+0.06}_{-0.05}$	$0.95^{+0.05}_{-0.08}$...
$\xi_{*,E}$	0.01 ^a	0.01 ^a	θ_E
...
χ^2	57.76	32.10	...
DOF	43	41	...
χ^2_ν	1.34	0.783	...

Note. — Parameter values for the no-parallax fit refer to a heliocentric frame; those for the parallax-included fit refer to a geocentric frame. Uncertainties are quoted at the $\Delta\chi^2 = 1$ level.

^afixed

^bHJD-2452000

Table 2. Parameters of best fit double source model

Quantity	No-parallax best fit value	Parallax included best fit value	Units
π_E	0.0 ^a	$1.4^{+0.3}_{-0.4}$	AU ⁻¹
ψ	0.0 ^a	$0.07^{+0.12}_{-0.20}$	rad
$f_{bl,1}$	0.28 ± 0.03	0.34 ± 0.04	...
u_0	0.23 ± 0.02	0.28 ± 0.03	r_E
t_0	775.4 ± 0.1	775.3 ± 0.2	days ^b
t_E	44 ± 2	41^{+3}_{-2}	days
$f_{bl,2}$	0.33 ± 0.04	$0.28^{+0.07}_{-0.05}$...
a	2.4 ± 0.1	$2.3^{+0.2}_{-0.1}$	r_E
ϕ	-0.046 ± 0.005	$0.03^{+0.03}_{-0.04}$	rad
...
χ^2	44.45	27.95	...
DOF	43	41	...
χ^2_ν	1.03	0.682	...

Note. — Parameter values for the no-parallax fit refer to a heliocentric frame; those for the parallax-included fit refer to a geocentric frame defined by the position and velocity of Earth near the time t_0 . Uncertainties are quoted at the $\Delta\chi^2 = 1$ level.

^afixed

^bHJD-2452000